CONSISTENCY OF THE DIVERTOR AND CORE PLASMA DENSITIES FOR BURNING PLASMAS

M.A. MAHDAVI,[1] V.S. CHAN,[1] R.J. GROEBNER,[1] M.E. FENSTERMACHER,[2]
T.H. OSBORNE,[1] A.W. LEONARD,[1] T.W. PETRIE,[1] and G.D. PORTER[2]

[1]General Atomics, P.O. Box 85608, San Diego, California 92186-5608

[2]Lawrence Livermore National Laboratory, Livermore, California

Abstract—ITER studies [1] show that increasing the line average density at constant β above the Greenwald limit increases the fusion power. The extent to which density can be increased is constrained by thermal instabilities in the core and divertor, H to L back transitions, and effects of density on confinement. Recent results from DIII–D [2–6], ASDEX Upgrade [7], and JET [8] show that operating at densities above the Greenwald limit is consistent with high confinement H–mode. Thus the main concern is consistency of the core density with safe divertor operation. Reducing the divertor heat load to an acceptable level requires a minimum separatrix density for achieving partial detachment of the divertor. However, with gas fueling, the density window between partial detachment and the divertor power balance limit is narrow [10] and excessive divertor density causes a back transition from H– to L–mode. Here, we address the problem of consistency of the divertor and core plasma densities in burning plasmas. Theoretical modeling [6] supported by DIII–D data show that with gas fueling alone, the separatrix density increases nonlinearly with the pedestal density; thus the detachment and the divertor power balance points can be reached before the desired core density is accessed. However, the coupling of the pedestal and separatrix densities can be broken by alternative fueling techniques combined with divertor pumping. It is proposed to fuel the plasma by a stream of small pellets, launched from the high field side.

INTRODUCTION

Normally in reactor studies, the divertor and core plasma problems are studied independently. In particular, in many divertor studies the density at the separatrix is set at a fixed fraction of the line average density, while the divertor geometry is varied to minimize the divertor heat flux. This approach can incorrectly lead to a closed divertor as the optimum design; whereas for achieving high densities at high confinement an open divertor might be superior. In recent papers [6] we pointed out that experiment shows that H–mode confinement degradation is correlated with the divertor power balance/detachment. Thus divertor power balance sets a practical upper bound on the separatrix density. Since in gas fuelled discharges the pedestal density is tightly coupled to the separatrix density [6], divertor power balance also limits the pedestal density. If this pedestal density is lower than the optimum core density for power production, then optimizing the divertor for detachment is counter productive. This is due to the fact divertor closure localizes the core particle source to the vicinity of X–point location, which has been shown [6] to reduce the ratio of the core to separatrix density.

Fueling by techniques with deeper particle deposition than gas fueling can significantly increase the ratio of the pedestal to separatrix density and thus increase the achievable high confinement density. Pellet injection combined with divertor pumping has been shown to be to effective in present machines [2,3,11,12]. However, it has been observed that large pellets trigger tearing modes and ELMs [3]. A possible technique, that has not been yet been adequately investigated, is to inject small pellets that penetrate just beyond the H–mode pedestal. This approach requires a high injection rate from the low field side. Another possible approach is injection of particles by a low energy neutral beam [6]. Both of these alternate fueling techniques involve complicated engineering issues and are more costly than gas fueling. Therefore, it is important to optimize the design for effective gas fuelling and introduce alternate techniques only if gas fueling is significant.

In this paper we will use a theory-based scaling method to predict the highest achievable pedestal densities in ITER-FEAT. There are six steps involved in the method used here:

1. A theoretical model is used to obtain a relation ship between the separatrix and pedestal densities.
2. The free parameters in the model are eliminated by fitting the model to experimental DIII–D data.
3. With a particle diffusivity scaling similar to the ITER confinement scaling $\tau_{IP898\text{-}Y2}$ [1], a relationship between the separatrix and the pedestal densities is obtained for the ITER-FEAT device.
4. A one-dimensional model of the divertor is developed to determine the scaling of the divertor power balance density limit.
5. The coefficient in front of the power balance scaling is determined by normalizing to data from a DIII–D discharge at the threshold of the divertor power balance limit.
6. The power balance separatrix density limit for ITER-FEAT is determined from step 5 and combined with results of step 3.

GAS FUELING MODEL

In this section we extend the gas fueling model developed by Engelhardt, Wagner and Mahdavi [13–15,6]. Our starting point is the particle diffusion equation given in Ref. [6]:

$$\frac{d^2 n_e}{dx^2} = \frac{S_i f(\theta_o)}{2V_n} \frac{\partial\left(n_e^2\right)}{\partial x} \quad , \tag{1}$$

for the region x<0, inside the separatrix, with the solution

$$n_e(x) = n_{PED} \tanh\left[C - \frac{S_i f(\theta_o)}{2V_n} n_{PED} x \right] \quad , \tag{2}$$

where $S_i = \langle \sigma_i v_e \rangle$ is the ionization rate, $f(\theta_o) = \dfrac{\left.\dfrac{\partial \psi}{\partial x}\right|_{\text{measurement location}}}{\left.\dfrac{\partial \psi}{\partial x}\right|_{\text{source}}}$, V_n is the average radial velocity of neutrals crossing the separatrix, and C is an integration constant.

The integration constant C is determined by requiring particle flux continuity at the separatrix

$$D_{CORE} \left.\frac{\partial n_e}{\partial x}\right|_{x=-o} = D_{SOL} \left.\frac{\partial n_e}{\partial x}\right|_{x=+o} \quad , \tag{3}$$

which results in

$$C = 0.5 \sinh^{-1}\left[\sqrt{D_{SOL}\tau_{\|}}\, \frac{S_i}{V_n} f(\theta_o) n_{PED} \frac{D_{CORE}}{D_{SOL}} \right] \quad . \tag{4}$$

for the region x>0, outside the separatrix, we use the Vokomizo model [?]:

$$n_e(x) = n_{SEP} e^{-\frac{x}{\sqrt{D_{SOL}\tau_{\|}}}} \quad , \tag{5}$$

At high densities, through charge exchange (CE) interactions, the velocity distribution of neutrals is expected to be similar to that of the local ions. Thus,

$$V_n \to V_{CE} = \frac{\int_o^\infty V_x f(V_x) dV_x}{\int_o^\infty f(V_x) dV_x} = \sqrt{\frac{T_i}{2\pi M_i}} \quad . \tag{6}$$

At low densities, neutrals reaching the separatrix are dominantly the Frank-Condon (FC) particles with an average energy of E_{FC} ~ 3 eV, and an average radial velocity $V_{FC} \cong \frac{2}{\pi}\sqrt{\frac{E_{FC}}{M_i}}$.

Since within an ionization mean free path half of the FC particles charge exchange, of which one-half travel radially inward, then the average forward velocity of neutrals is $V_n^* \cong \frac{S_i V_{FC} + S_{CE} V_{CE}/2}{S_i + S_{CE}/2}$. Although we are mainly concerned with the high density

limit where $V_n \approx V_{CE}$ is a good approximation, for the purpose of comparing the model with experimental data, it is important to know the transition point from the low to high density regime. For an estimate of the transition point we calculate W, the ratio of CE to FC neutrals reaching the separatrix by solving continuity equations for the FC and CE particles.

$$\nabla \bullet \left(n_{FC} V_{FC}\right) = -n_{FC} n_e S_i - n_{FC} n_e S_{CE} \quad , \tag{7}$$

$$\nabla \bullet \left(n_{CE} V_{CE}\right) = \frac{1}{2} n_{FC} n_e SCE - n_e n_{CE} S_i \quad , \tag{8}$$

where S_i and S_{CE} are the ionization and charge exchange rates, respectively, n_e is the divertor density, calculated from a 1-D, 2 point SOL model transport model [19].

The average neutral velocity is then approximated by

$$\overline{V_n} \cong \left(V_{CE} W + V_n^*\right) \Big/ (W + 1) \quad . \tag{9}$$

There are three free parameters in the problem: $f(\theta_o)$, D_{CORE}, and D_{SOL}. Of these the most significant one is $f(\theta_o)$ for determining the shapes of the density profile. This is demonstrated in Fig. 1 where we have varied the three parameters separately. At moderately high densities and low densities the width of the pedestal is determined primarily by $f(\theta_o)$. At very large densities, much of the density rise is in the SOL, and therefore D_{SOL} becomes important when $n_{PED} \gtrsim 8 \times 10^{19}$ m^{-3}.

Inside the separatrix the profile is not sensitive to either D_{SOL} or D_{CORE}. The main leverage of these two quantities is on the transition region since filtering of the Frank-Condon neutrals is sensitive to the SOL density.

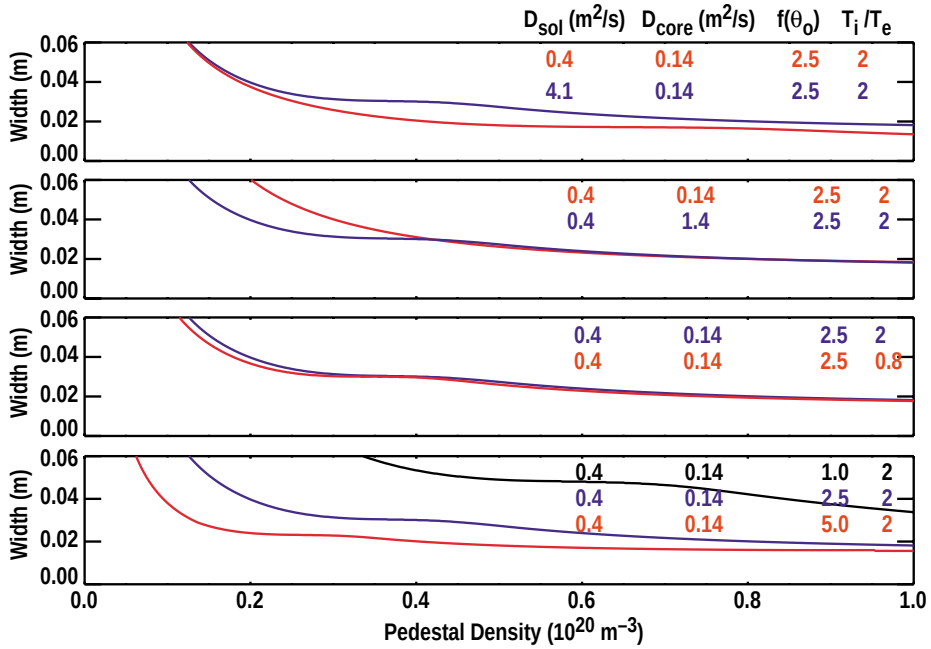

Figure 1. Sensitivity of the calculated density pedestal width to free parameters in the model. At moderately high densities the width of density profile is insensitive to diffusivities in the SOL and core and the ratio of T_i/T_e. The largest chage is observed when $f(\theta_0)$ is varied between 1 and 2.5. Although the profiles of T_i and T_e are measured within the pedestal, with the density rise the ratio of T_i/T_e decreases from separtrix to the pedestal top.

COMPARISON OF SOL MODEL WITH EXPERIMENTAL DATA

We have conducted an experiment in which the shape of the plasma, and the plasma was kept constant while the pedestal density was varied over a wide range by a combination of divertor pumping and gas fueling. The density profiles were measured by a Thomson scattering diagnostic system. The experimental data were then fitted to a hyperbolic tangent distribution [17]. The full width of this distribution was then compared to the full width of the density profile as predicted by the model. A fit of the model to the experimental data is shown in Fig. 2. The fit is for a value of $f(\theta_o) = 2.5$, $D_{SOL} = 0.34$ m^2/s, $D_{CORE} = 0.14$ m^2/s. This value of $f(\theta_o)$ indicates that the gas fueling source is from a broad area in the vicinity of X–point. This conclusion is qualitively supported by DEGAS–UEDGE modeling [18].

LIMITS OF THE VALIDITY OF THE MODEL

In general Eq. (2) in not valid since it assumes that the velocity distribution of neutrals is invariant and that neutrals are free streaming. In reality the charge exchange

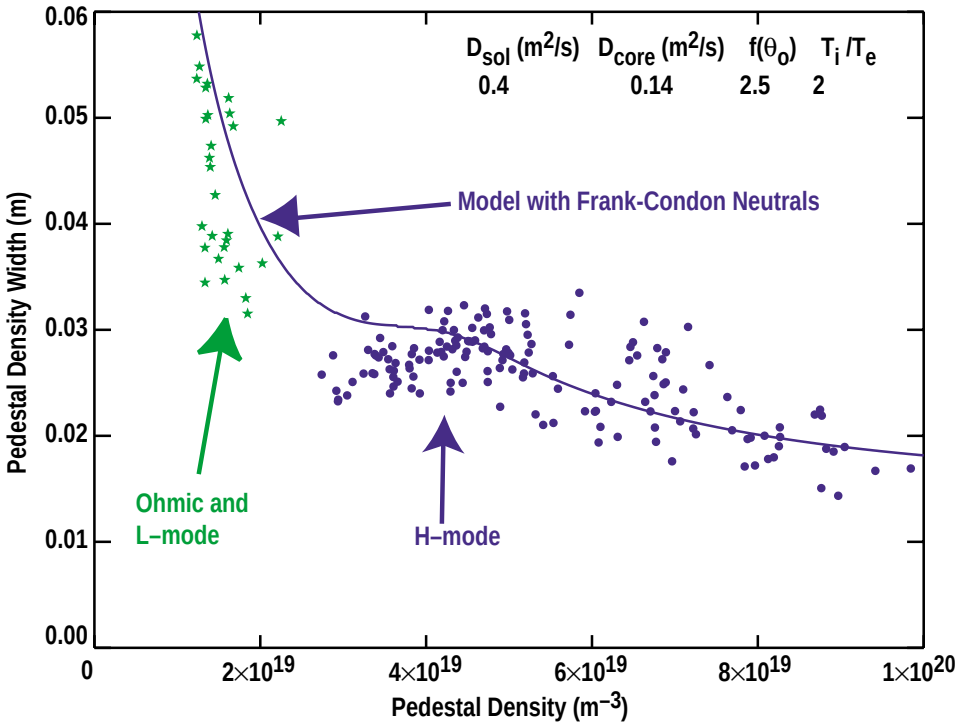

Figure 2. Comparison of the measure pedestal width and predictions of the model. The free parameters were varied for a good visual fit. Since the width of the profile is sensitive only to $f(\theta_0)$, this is the only parameter that is determined by this fit.

mean-free path, λ_{CE}, can be much shorter than ionization mean free path, λ_{ion}. Thus charge exchange collisions can change neutral penetration by causing changes in their velocity distribution or simply reduce neutral penetration through random scattering processes. Only for a limited temperature range, 40–500 keV, the ionization rate approaches the charge exchange rate. However if we restrict the use of the model to typical H–mode plasmas, then the electron temperature within the pedestal is within this range and on average only one charge exchange event takes place for each ionization event. This results in reducing the mean neutral penetration by only 20%. The second issue is variations in the ratio S_i/V_n within the density pedestal. If we apply the model to moderate density H–mode plasmas, then this ratio, is nearly constant within the density profile, while the electron temperature increases by a factor of two or more.

SOL MODEL

In this section we will derive the dependence of the divertor power blance density limit on the device parameters. The results are then used to determine the divertor power balance density limit for ITER-FEAT, by scaling from a high density DIII–D discharge. For this purpose we calculate the divertor parameters, using a 1-D model of the SOL allowing only electron thermal conduction and radiation. However, we allow δ, the width of the SOL, to change by requiring that 1/2 of P_s, power crossing the separatrix surface, is transported along the field lines and the balance of power to be transported radially. Accordingly, we have:

$$Q_\perp = \frac{1}{2} P_s = 2\pi^2 a R n_o \chi_\perp \frac{\partial T}{\partial n} \cong 2\pi^2 a R \frac{n_o T_o}{\delta} \quad , \tag{10}$$

$$q_\parallel^o = \frac{P_s q}{8\pi a^2 \delta} \quad , \tag{11}$$

$$\frac{\partial}{\partial x} q_\parallel = -L \quad , \tag{12}$$

$$q_\parallel = \kappa_o T^{5/2} \frac{\partial T}{\partial x} \quad , \tag{13}$$

$$n_d T_2 = 1/2\, n_o T_o \quad , \tag{14}$$

$$q_\parallel^o - \int_o^\ell L dx = \gamma \beta n_d T_d^{3/2} n_d T_d^{3/2} \quad , \tag{15}$$

where $q_\parallel^o$ is the safety factor, L is the emissivity of the plasma, γ is the sheath transmission coefficients, $\beta = \frac{c_s}{T^{1/2}}$. We define a quantity M, called the moment of radiation as

$$M \equiv \frac{\int_o^\ell \int_o^{x'} L(x') dx' dx}{\ell \int_o^\ell L(x) dx} \quad . \tag{16}$$

The magnitude of M is determined by $q_{\|}^{o}$ and the nature of the radiating impurity. The larger the value of M, the lower is the separtrix density at which the divertor power balance limit and detachment is reached. For a pure deuterium plasma M<<1, and for an uniform radiator $M = \frac{1}{2}$.

Let $\chi_{\perp} \equiv \chi T^{m}$, so that the temperature dependence of $\chi_{\perp}$ can be expressed explicitly. Later for Bohm diffusion, we will substitute m=1 and $\chi \propto \frac{1}{B_T}$, and for a constant SOL width δ, m=–1 and $\chi \propto \frac{P_s}{n_o a R}$.

Then we obtain

$$T_o = \left[\frac{(1 - Mf_r)}{9.1\kappa_o \pi^2 a^2 x} \frac{P_s^2 q^2}{n_o} \right]^{\frac{2}{q+2+m}} , \tag{17}$$

$$\delta = \frac{4n^2 a R \chi n_o}{P_s} \left(\frac{P_s^2 q^2 (1 - Mf_r)}{9.1\kappa_o \pi^2 a^2 \chi n_o} \right)^{\frac{2m+2}{9+2m}} \tag{18}$$

$$\Gamma_D = \frac{n_o \gamma^q \beta^2}{4\left(q_{\|}^{o} - \int_o^{\ell} L dx \right)} \left(\frac{P_s^2 q^2 (1 - Mf_r)}{9.1\kappa_o \pi^2 a^2 \chi n_o} \right)^{\frac{4}{9+2m}} , \tag{19}$$

where f_r is the fraction of P_s, radiated in the SOL.

We notice that for Bohm-like diffusion, i.e., m=1, $\chi \propto \frac{1}{B_T}$, $\delta \propto \frac{n_o}{P_s^{3/11}} \frac{B_T^{1/11}}{I_p^{8/11}}$. Therefore, the SOL width increases with increasing upstream density and, decreases with increasing I_p and power.

For a pure deuterium plasma, $\int_o^{\ell} L dx$ can be approximated by $g\Gamma_d$, where g is approximately 30 eV. Using this approximation in Eq. (19), and solving for Γ_d, we obtain

$$\Gamma_d \cong \frac{1}{2g} \left(q_{\|}^{o} \pm \sqrt{q_{\|}^{o\,2} - 4gU} \right) , \tag{20}$$

where $U \equiv \frac{n_o^2 \gamma \beta^2}{4}\left(\frac{P_s^2 q^2}{9.1\pi^2\alpha^2\chi n_o}\right)^{\frac{4}{9+2m}}$.

In deriving the result of Eq. (20), we have approximated by setting $(1-Mf_r)^{\frac{4}{9+2m}} \approx 1$, since $f_r \le 1$ and $M < 0.5$.

The divertor power balance density limit is obtained by setting the quantity under the radical in Eq. (11) equal to zero:

$$n_o^{max} = \frac{\left(9.1\kappa_o\pi^2\alpha^2\right)^{\frac{m+2}{7+m}}}{\left[g\left(32\pi^2\right)^2\gamma\beta^2 a^4 R^2\right]^{\frac{9+2m}{28+4m}}}\left(\frac{P_s}{\chi}\right)^{\frac{5}{14+2m}} q^{\frac{1-2m}{14+2m}} \quad , \tag{21}$$

For Bohm-like diffusion, i.e., m=1, $\chi\alpha\frac{1}{B_T}$. We have

$$n_o^{max}(\text{Bohm}) \propto a^{-5/8} R^{-11/16} q^{-1/16} B_T^{5/16} P_s^{5/8} \quad , \tag{22}$$

For a constant SOL, width, m=–1, $\chi \propto \frac{P_s\delta}{aRn_o}$, we have

$$n_o^{max}(\text{constant } \delta) \propto a^{-5/7} R^{-2/7} q^{3/14} P^{5/7} \quad . \tag{23}$$

SCALING TO ITER-FEAT

We are now in a position to determine the achievable highest pedestal density in ITER-FEAT by scaling from gas fueled high density DIII–D H–mode plasmas. For this purpose, we have chosen the highest density discharges of Fig. 2. These discharges have an open configuration, and our basic assumption here is that ITER-FEAT can also be operated in a similar open configuration. Using the scalings of Eqs. (22) and (23) we obtain limiting separatrix densities for ITER-FEAT relative to the DIII–D discharges. The high density DIII–D discharges of Fig. 2 have a separatrix density of $2\times10^{19} m^{-3}$ (for example see discharge 98893 [5]). Since attempts to increase the plasma density beyond this point result in confinement degradation, we assume that

$2\times10^{19}\mathrm{m}^{-3}$ represents the highest separatrix density for a gas fueled discharge in this open configuration, heating power, and current. Using this value of the separatrix density, we obtain the corresponding separatrix densities for ITER-FEAT for the two different SOL models. Finally, using the best fit parameters of Fig. 2, and $\mathrm{ITER}_{98\text{-}Y2}$ scaling for the diffusivities, we obtain the respective maximum pedestal densities for ITER-FEAT. These results are summarized in Table 1 and Fig. 3. These results show that in all cases studied the pedestal density can reach or exceed the Greenwald limit.

TABLE 1
Highest Achievable Pedestal Densities in ITER-FEAT are Calculated by Scaling from the DIII–D Discharge 98893

	DIII–D	ITER
R (m)	1.7	6.2
a (m)	0.59	2.0
P_s (MW)	3	75/150
q	3.1	3.1
$\left.\frac{n_o}{n_{o(98893)}}\right\|_{\text{const. }\delta}$	1	2.9/4.8
$\left.\frac{n_o}{n_{o(98893)}}\right\|_{\text{Bohm}}$	1	2.1/3.2
$n_{PED}\|_{\text{const. }\delta}\ \left(10^{20}\,\mathrm{m}^{-3}\right)$	0.9	1.3/1.65
$n_{PED}\|_{\text{Bohm}}\ \left(10^{20}\,\mathrm{m}^{-3}\right)$	0.9	1.1/1.3

CONCLUSIONS AND DISCUSSION

Divertor power balance sets an upper limit on the highest achievable pedestal density. We have calculated the highest achievable density in ITER-FEAT, based on this consideration alone, ignoring other density limiting processes. The results summarized in Table 1 show that pedestal densities close to or exceeding the

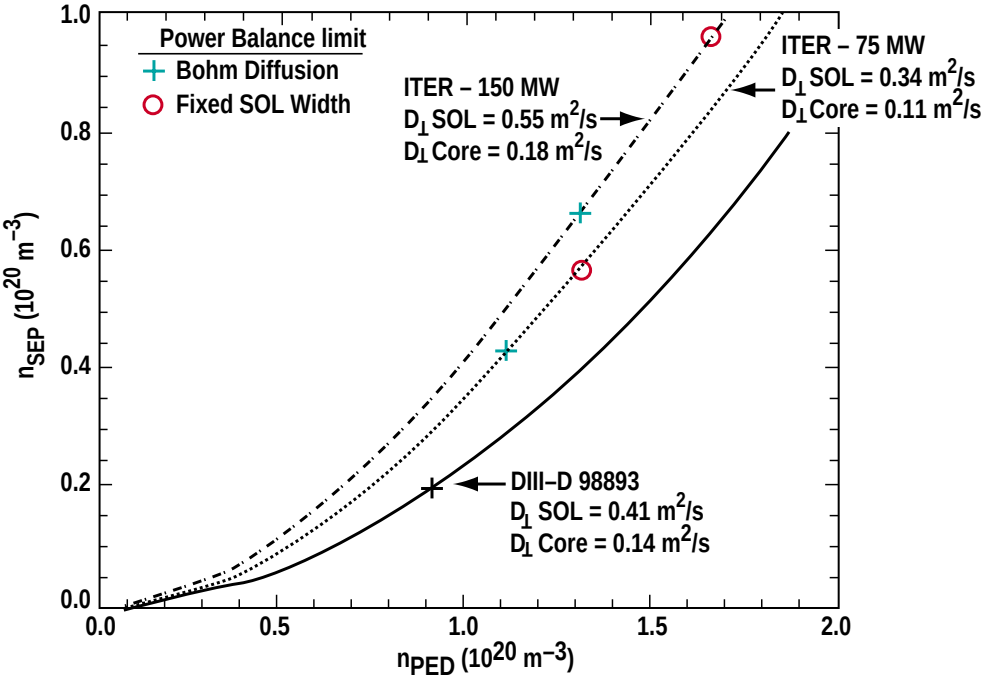

Figure 3. Separatrix density versus pedestal density for calculate for DIII–D and ITER-FEAT at two heating powers. The divertor power balance density limits are marked for two SOL models; Bohm diffusion (Bohm Diffusion) and constant SOL width (open circles). The black cross on the DIII–D curve shows a readily accessible pedestal density in the configuration of the discharge 98893.

Greenwald limit (~ 1.2×10^{20} m^{-3}) are achievable, with gas fueling alone if an open divertor configuration similar to the DIII–D discharge 98893 is utilized. Even with a flat density profile, such a high pedestal density should be adequate for ITER-FEAT goals. However, because of uncertainties in the models used here and other technical considerations that might preclude an open configuration, it is prudent to develop a neutral source that deposits particles beyond the H–mode pedestal. A low energy neutral beam has been proposed [6] for this purpose. A low neutral beam has the advantage of also injecting copious quantities of toroidal angular momentum that can enhance the edge transport barrier. However low energy neutral beam sources require large access ports. Another possibility is injection of a stream of small pellets. The key issue for pellets is that pellets have to be small enough so that its density perturbation is small enough not to trigger ELMs, tearing modes or radiative instabilities. This might be technically possible if the pellets are required to penetrate only just beyond the H–mode pedestal.

Acknowledgment—Work supported by U.S. Department of Energy under Contracts DE-AC03-99ER54463, W-7405-ENG-48, and DE-AC02-76CH03073.

REFERENCES

[1] ITER physics basis, Nucl. Fusion, Vol 39 (1999) 2599.

[2] M.A. Mahdavi, *et al*., IAEA-CN-641A4-3 (1996) 397.

[3] R. MAINGI, *et al*., Phys. Plasmas **4** (1997) 1752.

[4] M.A. MAHDAVI, *et al*., Controlled Fusion and Plasma Phys. **21** (1997) 1113.

[5] T. Osborne, J. Nucl. Mater. 290-293 (2001) 1013.

[6] M.A. Mahdavi, *et al*., "High Performance H–mode Plasmas at Densities Above the Greenwald Limit," to be published in Nucl. Fusion.

[7] J. Stober, *et al*., Proc. of EPS (2000).

[8] M. Valovic, *et al*., to be presented at the EPS conference, Madeira, Portugal.

[9] T.Carlstrom, *et al*., physics of plasmas 3 (1996) 1867.

[10] T. Petrie, Journal of Nucl. Mater, 241-243 (1997) 639.

[11] TEXTOR.

[12] ASDEX.

[13] W. ENGLEHARDT, W. FENEBERG, J. Nucl. Mater. **76-77** (1978) 518.

[14] F. WAGNER, K. LACKNER, "Phys. Plasmas – Wall Interactions in Controlled Fusion," Nato. ASI Series B, Physics Vol. 131, p. 931.

[15] P. STANGEBY, "The Plasma Boundary of Magnetic Fusion Devices," Inst. of Phys. Publishing, Bristol (2000) p. 175.

[16] H. YOKOMIZO, *et al*., Plasma Phys. and Contr. Nuclear Fusion Research 1982, Vol. III, IAEA, Vienna (1983) p. 173.

[17] R.J. Groebner, and T.N. Carlstrom, 40, (1998) p. 673.

[18] L.W. OWENS, Private communications.